Heterogeneous Catalytic Deoxygenation of Stearic Acid for Production of Biodiesel

Mathias Snåre, Iva Kubičková, Päivi Mäki-Arvela, Kari Eränen, and Dmitry Yu. Murzin*

Laboratory of Industrial Chemistry, Process Chemistry Centre, Åbo Akademi University, Biskopsgatan 8, FIN-20500 Turku/Åbo, Finland

A novel method for production of diesel-like hydrocarbons via catalytic deoxygenation of fatty acid is discussed. The model compound stearic acid is deoxygenated to heptadecane, originating from the stearic acid alkyl chain. The deoxygenation reaction is carried out in a semibatch reactor under constant temperature and pressure, 300 °C and 6 bar, respectively. A thorough catalyst screening was performed to obtain the most promising metal and support combination. The catalysts were characterized by N_2-physisorption, CO-chemisorption, and temperature-programmed desorption of hydrogen. A highly active and selective in the deoxygenation reaction of stearic acid carbon supported palladium catalyst converted stearic acid completely with >98% selectivity toward deoxygenated C17 products.

Introduction

The increasing consumption of fuel in the previous decades has led to a rapid decrease of Earth's fossil reservoirs; therefore, innovative solutions for future fuel should be made. Fuels derived from renewable recourses, such as biomass, are favorable alternatives.[1] At the moment, a common and highly functional fuel with high combustion efficiency[2] is the diesel fuel.

In this paper, a novel method for production of biodiesel, in the form of diesel fuel hydrocarbons, will be presented. Production of diesel fuels from renewable resources is mainly done via a transesterification reaction[3−5] but can as well be performed via pyrolysis and/or deoxygenation reactions.[6,7] The deoxygenation of vegetable-based feeds is typically related to pyrolysis (cracking), where the hydrocarbon chain is broken and the oxygen is removed. The drawback of this approach is the loss of carbon and decreasing energy content of the produced fuel. The selective production of diesel fuel hydrocarbons from renewable vegetable-based feeds was recently reported, where the deoxygenation was performed by selective removal of the carboxyl group.[8]

The main aim of this study is to deoxygenate fatty acids, through decarboxylation and/or decarbonylation resulting in straight-chain hydrocarbons. Plausible reaction paths for production of linear hydrocarbons from fatty acids are illustrated below (thermodynamic data for production of linear C17 hydrocarbons from stearic acid are provided for 300 °C).

Liquid phase reactions

					ΔG_{573} (kJ/mol)	ΔH_{573} (kJ/mol)
I.	Decarboxylation:	R-COOH	→	R-H + CO_2 (g)	-83.5	9.2
II.	Decarbonylation:	R-COOH	→	R´-H + CO (g) + H_2O (g)	-17.0	179.1
III.		R-COOH + H_2 (g)	→	R-H + CO (g) + H_2O (g)	-67.6	48.1
IV.	Hydrogenation:	R-COOH + $3H_2$ (g)	→	$R\text{-}CH_3$ + $2H_2O$ (g)	-86.1	-115.0

R = saturated alkyl group *R´ = unsaturated alkyl group*

There are several possible reaction paths for production of straight-chain hydrocarbons. Fatty acids can be directly decarboxylated or decarbonylated. Direct decarboxylation removes the carboxyl group by releasing carbon dioxide and producing a paraffinic hydrocarbon, while direct decarbonylation produces an olefinic hydrocarbon via removal of the carboxyl group by forming carbon monoxide and water, as illustrated by reactions I and II. Additionally, the fatty acid can be deoxygenated by adding hydrogen; in this case, the production of linear hydrocarbon can occur via direct hydrogenation or indirect decarbonylation, reactions III and IV, respectively. As the catalytic deoxygenation in the present study is carried out under inert atmosphere, reactions III and IV are of minor importance.

Additionally to the liquid-phase reactions, there are a number of reactions occurring with CO, CO_2, hydrogen, and water formed during decarboxylation/decarbonylation, in particular water gas shift and methanation (reactions V−VII; thermodynamic data for gas-phase reactions are provided for 300 °C).

Gas phase reactions

					ΔG_{573} (kJ/mol)	ΔH_{573} (kJ/mol)
V.	Methanation:	CO_2 + $4H_2$	⇌	CH_4 + $2H_2O$	-61.2	-177.2
VI.	Methanation:	CO + $3H_2$	⇌	CH_4 + H_2O	-78.8	-216.4
VII.	Water-gas-shift	CO + H_2O	⇌	H_2 + CO_2	-17.6	-39.2

More than 80 years ago, Bertram[9] succeeded to decarboxylate stearic acid to heptadecane by a homogeneous catalytic reaction over selenium. The paraffin yield of just 50% was, however, obtained, and simultaneous dehydrogenation of produced paraffin to olefin was observed. Much later, Foglia and Barr[10] demonstrated conversion of fatty acids to alkenes by a homogeneous catalytic reaction with complexes of palladium and rhodium.

The heterogeneous catalyzed deoxygenation of vegetable-based feeds has been studied scarcely in the past (with the exception of cracking). Decarboxylation of aliphatic and aromatic carboxylic acids was carried out in the gas phase over Pd/SiO_2 and Ni/Al_2O_3.[11] The experimental results showed that Pd/SiO_2 catalyst gave a much higher yield in decarboxylating heptanoic and octanoic acid (98% and 97%, respectively) than that achieved over the Ni/Al_2O_3 catalyst (26% and 64%, respectively). Production of straight-chain olefins from saturated fatty acids and fatty acid esters over a nickel based catalyst promoted with either tin, germanium, or lead was a subject of a patent.[12] In the field of biomass conversion, a similar catalytic deoxygenation reaction over a metal alloy (RuPd) supported on a carbonaceous material was reported.[13] The present paper

* Corresponding author. E-mail: dmurzin@abo.fi.

10.1021/ie060334i CCC: $33.50
Published on Web 06/28/2006

Table 1. Tested Catalysts

	catalyst						reduction conditions		
	metal	support	code	metal content (%)	manufacturer	type	ramp (°C/min)	temp (°C)	time (min)
1	nickel	(Raney, skeletal)	81% Raney-Ni	81	H. C. Starck	commercial (5584S)			
2	nickel	aluminum oxide	16% Ni/Al_2O_3	16	Crossfield	commercial (HTC 400)	5	360	240
3	nickel	silicon oxide	60% Ni/SiO_2	60	Strem Chemicals	commercial (28−143)	5	360	240
4	nickel	chromium oxide	50% Ni/Cr_2O_3	50	Chirchik	commercial	5	360	240
5	nickel & molybdenum	aluminum oxide	3%,9% $NiMo/Al_2O_3$	12	AKZO	commercial	5	360	240
6	rutenium	silicon oxide	5% Ru/SiO_2	5	Åbo Akademi	self-synthesized	5	200	120
7	rutenium	magnesium oxide	5% Ru/MgO	5	Åbo Akademi	self-synthesized	5	200	120
8	rutenium	activated charcoal	5% Ru/C	5	Fluka	commercial (84031)	5	200	120
9	palladium	aluminum oxide	5% Pd/Al_2O_3	5	Åbo Akademi	self-synthesized	5	200	120
10	palladium	activated carbon	1% Pd/C	1	Alfa	commercial (89113)	5	200	120
11	palladium	activated carbon	10% Pd/C	10	Aldrich	commercial (20.569-9)	5	200	120
12	palladium	activated carbon	5% Pd/C	5	Aldrich	commercial (20.568-0)	5	200	120
13	palladium & platinum	activated carbon	8%,2% PdPt/C	10	Johnson Matthey	commercial (10R464/45)	5	200	120
14	platinum	aluminum oxide	5% Pt/Al_2O_3	5	Strem Chemicals	commercial (78-1660)	5	200	120
15	platinum	activated carbon	5% Pt/C	5	Johnson Matthey	commercial (5R18/264)	5	200	120
16	iridium	aluminum oxide	2% Ir/Al_2O_3	2	Åbo Akademi	self-synthesized	1	250	480
17	iridium	silicon oxide	1% Ir/SiO_2	1	Åbo Akademi	self-synthesized	1	250	480
18	osmium	activated carbon	5% Os/C	5	Karpov Institute	self-synthesized	5	200	120
19	rhodium	silicon oxide	3% Rh/SiO_2	3	Karpov Institute	self-synthesized	5	200	120
20	rhodium	activated carbon	1% Rh/C	1	Johnson Matthey	commercial (89925)	5	200	120

focuses on a variety of supported metal catalysts and their testing in stearic acid decarboxylation.

Experimental Section

Screened Catalyst. A thorough catalyst screening was done with supported monometallic and bimetallic catalysts as well as with a skeletal nickel catalyst. The metals studied were Ni, Mo, Pd, Pt, Ir, Ru, Rh, and Os on Al_2O_3, Cr_2O_3, MgO, and SiO_2 as well as on activated carbons. Mainly commercial catalysts were used, but additionally, self-synthesized catalysts were tested. Ru/SiO_2, Ru/MgO, Ir/Al_2O_3, and Ir/SiO_2 catalysts were synthesized by impregnation with chlorine containing precursor, while for Pd/Al_2O_3 synthesis, palladium nitrate was used. The Rh/SiO_2 and Os/C catalysts were prepared at Karpov Physico-Chemical Institute in Moscow.[14] Other carbon supported metal catalysts such as Pd and Pt were provided by Aldrich and Johnson Matthey.

Catalyst Pretreatment. The particle sizes of the commercial powder catalysts were below 50 μm, whereas the self-synthesized catalysts were sieved, normally below 63 or 90 μm, to minimize the effect of internal mass transfer limitations. The catalysts were dried in an oven for 4 h at 105 °C prior to catalyst reduction and subsequent reaction. Typically the catalyst (1 g) was placed in the reactor and reduced in situ by flowing hydrogen (30 mL/min) at 200 kPa. The temperature ramp was 1 or 5 °C/min until reaching the reduction temperature, normally between 200 and 360 °C, at which the catalyst was reduced for 2−8 h. After the reduction, the reactor was thoroughly flushed with an inert gas in order to remove excessive hydrogen. A summary of investigated catalysts is presented in Table 1.

Catalyst Characterization. The catalysts were characterized by acidity measurements of the aqueous catalyst slurries, nitrogen physisorption, temperature-programmed desorption of hydrogen, and CO-chemisorption.

Surface area measurements were conducted with the physisorption/ chemisorption instrument Sorptometer 1900 (Carlo Erba instruments).The specific surface area was calculated according to the Brunauer−Emmett−Teller (BET) isotherm with the exception of the microporous and mesoporous carbon supports, which were treated using the Dubinin−Radushkevich equation. The pore size distribution was obtained from the Dollimore−Heal correlation.

The catalysts were studied by temperature-programmed desorption of hydrogen (TPD-H_2) using an Autochem 2910 apparatus (Micromerics). The catalyst was placed into a U-tube and heated by a flow of hot inert gas (helium) to reduction temperature. After reaching the reduction temperature, the flow of inert gas was replaced by a hydrogen flow for 2 h, followed by cooling to room temperature and flushing in inert gas. The sample was then heated 10 °C/min under a constant volumetric flow (50 mL/min) of inert gas to 700 °C; this temperature was then kept constant for 60 min. The desorbed gases were detected by a quadropole mass spectrometer (QTMD, Carlo Erba instruments).

Determination of the metal dispersion was carried out by using the Autochem 2910 apparatus (Micromerics) as mentioned above. The dispersion was measured by CO-chemisorption. The sample (ca 0.2 g) was placed into the U-tube and reduced by hydrogen (20 mL/min) while increasing the temperature linearly, 5 °C/min to 200 °C, where it was kept for 2 h. After the reduction, the catalyst sample was cooled to 40 °C under helium flow. The chemisorption of CO was then achieved by pulsing CO through the system and saturating the catalyst completely. The stoichiometric relationship between metal (Pt and Pd) and CO is assumed to be unity.[15]

The measurements of catalyst acidity were performed with a pH electrode (Metroohm) in an aqueous catalyst slurry. The catalyst slurry was stirred with a magnetic stirrer, while pH was monitored and registered. The acidity was determined after reaching a constant pH value.

Deoxygenation Experiments. The catalytic experiments were carried out in a 300 mL semibatch reactor coupled to a condenser and a heating jacket. The overall pressure and the temperature were kept constant at 600 kPa and 300 °C, respectively. Stirring speed was maintained suitably high, 1100 rpm, to prevent external mass transfer limitations. Preliminary experiments over 5% Pd/C with different stirring speeds proved that 1100 rpm was sufficiently high for the examined system. The flow of carrier gas and the reaction pressure were controlled by a flow controller (Brooks 58505S) and a pressure controller (Brooks 5866), respectively. The reaction temperature and the pressure profiles were monitored and registered.

The model compound stearic acid ($C_{18}H_{36}O_2$), of 97% purity, was supplied by Acros Organics. The reaction and the reduction

gases, helium (99.996%) and hydrogen (99.999%), were provided by AGA. The solvent, dodecane ($C_{12}H_{26}$), was supplied by Fluka and Aldrich, with 98% and 99% purity, respectively. The chemicals were used as received.

Catalyst reduction was followed by introduction of 86 g of the solvent, dodecane, into the reactor via a bubbling unit preventing reoxidation of the catalyst. In the bubbling unit, the solvent was heated to 45 °C to make it less viscous, thus avoiding solvent losses when transferred to the reactor. After solvent introduction, the reactor was opened and 4.5 g of stearic acid (0.154 mol/L) was placed into it. Thereafter, the reactor was flushed thoroughly with inert gas (helium, 25 mL/min), and the pressure was adjusted to 600 kPa prior to reaction. The reaction mixture was then heated with a temperature rate of 15 °C/min to 300 °C, and at this point, stirring and reaction time was started. The spent catalyst particles were filtered with 200 mL of acetone after the reaction and characterized by nitrogen adsorption.

Product Analysis. Several liquid-phase samples were withdrawn from the reactor via a sampling valve during the experiments. Typically, samples had to be dissolved in pyridine and silylated with *N*,*O*-bis(trimethyl)trifloroacetamide, BSTFA (Acros Organics, 98+%), in order to analyze in GC. Generally, 30 wt % pyridine and 100 wt % excess of BSTFA were added to the sample. After addition of silylation agent, the samples were kept in an oven at 60 °C for 30 min. The internal standard eicosane, $C_{20}H_{42}$ (Acros Organics, 99% of purity), was added for quantitative calculations. The samples were analyzed with a gas chromatograph (GC, HP 6890) equipped with a nonpolar column (DB-5, with dimensions of 60 m × 0.32 mm × 0.5μm) and a flame ionization (FI) detector. A sample (1 μL) was injected into the GC with a split ratio 50:1, and the carrier gas (helium) flow rate was 137 mL/min. The injector and detector temperatures were 265 and 290 °C, respectively. The following temperature program was used for analysis: 110 °C (1 °C/min), 126 °C (30 °C/min), 185 °C (1 °C/min), 200 °C (5 °C/min), and 300 °C (45 min). The chromatographic pressure program was well-adjusted to achieve satisfactory separation of the desired product, its isomers, and olefins. The initial pressure at 172.4 kPa was kept for 1 h, after which the pressure was ramped with 34.5 kPa/min until reaching the final pressure 221 kPa. A number of chemical standards (dodecane, hexadecane, *n*-heptadecane, 1-heptadecene, octadecane, eicosane, lauric acid, palmetic acid, stearic acid, and arachidic acid) were purchased, enabling product identification and calibration. The product identification was validated with a gas chromatograph−mass spectrometer (GC−MS). Quantitative calculations were performed by the normalization method and supplemented by using the internal standard (eicosane) method.

Gas-phase analysis was conducted in situ for selected experiments to attain necessary information about reaction pathways. The gas composition was determined by a GC (Microlab Aarhus) coupled with a thermal conductivity (TC) detector. The compound identification and calibration were performed with calibration gases (1 vol % CO_2, 1 vol % C_2H_6, 0.1 vol % C_2H_4, 1 vol % CH_4 in helium and 203 ppm_{mol} CO_2, 1 mol % CO in helium) supplied by AGA. The peak areas were integrated with the software Star Variant. Helium was used as a carrier gas. The chromatograph was equipped with a HP-PLOT molecular sieve and GS-Q column (30 m × 0.534 mm). The injector and detector temperatures were kept at 20 and 200 °C, respectively. The oven temperature was isothermal at 20 °C. Complete quantification of the obtained information remains, however, challenging because of the nonconstant flow of the outlet gas.

Table 2. Specific Surface Areas and Particle Sizes of Tested Catalysts

			particle size	
catalyst	surface area (m^2/g)	sieving (μm)	mean (μm)	<50 μm (%)
81% Raney-Ni	94		7.0	100
16% Ni/Al_2O_3	105	<90	11.9	100
60% Ni/SiO_2		<90	29.4	93.7
50% Ni/Cr_2O_3	88	<90	13.3	99.5
3%,9% $NiMo/Al_2O_3$	195	<90	16.8	98.4
5% Ru/SiO_2	411	<90	52.9	44.5
5% Ru/MgO		<90	13.9	99.5
5% Ru/C	841		19.6	94.2
5% Pd/Al_2O_3	299[b]	<90	18.5	97.9
1% Pd/C	1126(1429)[a]		29.9	77.6
10% Pd/C	782(996)[a]		30.4	83.9
5% Pd/C	936(1214)[a]		14.98	96.6
8%,2% PdPt/C			27.9	85.1
5% Pt/Al_2O_3	95		21.0	91.2
5% Pt/C	797(999)[a]		19.12	92.4
2% Ir/Al_2O_3	299[b]	<63	13.3	99.9
1% Ir/SiO_2	379[b]	<63	51.4	47.6
5% Os/C	610		24.7	94.7
3% Rh/SiO_2	490		39.8	81.1
1% Rh/C			16.1	99

[a] Number in brackets is the surface area calculated based on Dubinin−Radushkevich equation. [b] Surface area of supports (alumina and silica supplied by UOP and Merck, respectively).

Results and Discussion

Characterization Results. The catalyst surface areas and catalyst particle sizes of the utilized catalysts were determined and summarized in Table 2. The screened catalyst surface areas varied from the large surface area carbon supports (>1000 m^2/g) to the low surface area metal oxide supports (<100 m^2/g). The mean catalyst particle size was typically ~20 μm, and the majority of tested catalysts had the dominant fraction of particles below 50 μm, thus minimizing the effect of internal mass transfer limitations. More extensive characterization has been performed for Pd and Pt supported on carbon catalyst.

The CO-chemisorption measurements for palladium on carbon catalysts revealed that the metal dispersion decreased with the increase of the metal loading. Furthermore, specific surface areas decreased with the increase of metal loading. Nevertheless, the pore size distribution for the examined catalysts did not follow the same trend. 1% Pd/C and 5% Pd/C had larger micropore volumes than those for 10% Pd/C and 5% Pt/C and logically also a bigger relative amount of pores below 1 nm. The pH of the catalyst slurry indicated that 10% Pd/C and 5% Pt/C were slightly acidic, while 1% Pd/C and 5% Pd/C were alkaline (Table 3).

Temperature-programmed desorption of hydrogen showed that the desorbed amount of hydrogen at the reaction temperature 300 °C was higher for 10% Pd/C and PdPt/C than for 1% Pd/C, 5% Pd/C, and 5% Pt/C. 5% Pd/C had approximately double the amount of the total hydrogen desorbed per gram of catalyst compared to 1% Pd/C, while 10% Pd/C, 5% Pt/C, and 8%,2% PdPt/C had 7.6, 12.4, and 3.0 times higher, respectively, than 1% Pd/C (Table 4).

Deoxygenation Results. Thermal (noncatalytic) deoxygenation of stearic acid was performed in the absence of any catalyst for 6 h at a constant reaction temperature and reaction pressure, 300 °C and 6 bar, respectively. The extent of thermal deoxy-

Table 3. Palladium and Platinum Carbon Catalyst Properties

	catalyst acidity	CO-chemisorption		N_2-physisorption								
				surface area (m^2/g_{cat})				pore size distribution (%)				
catalyst	(pH_{slurry})	metal surface area (m^2/g_{met})	dispersion (%)	fresh	used	decrease (%)	micropore volume (mL/g_{cat})	<1 nm	1−2	2−5	5−10	>10 nm
1% Pd/C	8.7	120.3	27	1429	481	66.3	0.507	15.1	26.0	22.8	5.0	31.0
5% Pd/C	10.2	80.2	18	1214	509	58.1	0.431	11.3	31.1	30.0	6.5	21.1
10% Pd/C	4.9	62.4	14	996	403	59.5	0.353	3.1	30.4	36.2	15.2	15.1
5% Pt/C	6.7			999	402	59.8	0.355	4.1	22.8	22.5	16.0	34.7

Table 4. Results of Temperature-Programmed Desorption of Hydrogen over Palladium and Platinum

	H_2 TPD						
			peak I		peak II		
catalyst	desorbed H_2 at 300 °C[a]	$T_{peak\ separation}$ (°C)	relative area[a]	T_{max} (°C)	relative area[a]	T_{max} (°C)	total desorbed H_2[a]
1% Pd/C	0.3	305	0.28	245	0.72	379[b]	**1.0**
5% Pd/C	1.5	250	0.89	220[b]	1.59	304[b]	2.5
10% Pd/C	2.2	260	1.68	203[b]	5.88	489[b]	7.6
5% Pt/C	0.3	260	1.09	140[b]	11.32	419	12.4
8%,2% PdPt/C	2.3	180	0.78	162[c]	2.23	233[b]	3.0

[a] Relative to total amount of desorbed hydrogen from Pd(1%)/C. [b] Broad. [c] Very broad.

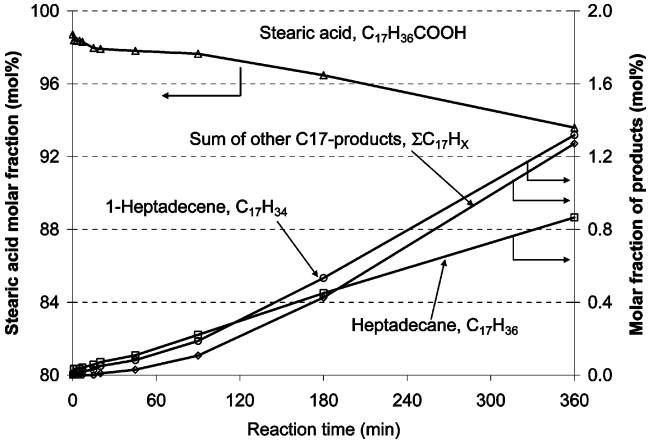

Figure 1. Thermal (noncatalytic) deoxygenation of stearic acid in dodecane. The reaction conditions are as follows: $m_{stearic\ acid} = 4.5$ g, $m_{dodecane} = 86$ g, $T = 300$ °C, $p = 6$ bar, and $V_{carrier\ gas} = 25$ mL/min (He).

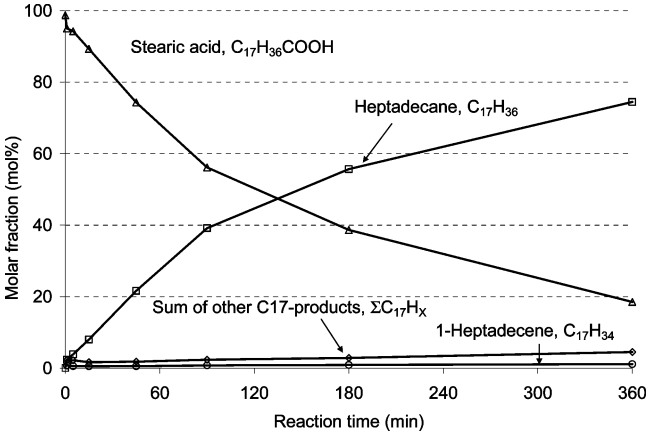

Figure 2. Reactant and product concentration profiles in the deoxygenation of stearic acid over 5% Ru/C. Reaction conditions are the same as in Figure 1, $m_{catalyst} = 1$ g.

genation under these conditions was minor; the results showed that <5% of stearic acid was converted within 6 h of reaction. The main products formed were linear C17 hydrocarbons, such as 1-heptadecene (26% of selectivity after 6 h) and *n*-heptadecane (17%). Additionally, other unsaturated C17 hydrocarbons (25% of selectivity), such as 3-heptadecene, 8-heptadecene, and undecylbenzene, were produced as well (Figure 1).

To separate the current study from the previous reported homogeneous catalytic deoxygenation (decarboxylation), an initial investigation of metal leaching to the liquid phase was conducted. Metal leaching analysis was performed by direct current plasma atomic emission spectroscopy (DCP-AES) of the reaction mixture after 6 h of reaction over a 5% Pd/C catalyst. The low palladium amount (>5 ppm_m) leached to stearic acid and dodecane proves that the catalytic reaction is taking place over the solid catalyst rather than being a homogeneous phenomenon.

The above-mentioned observation on the absence of external diffusion together with the absence of interparticular diffusion limitations based on the calculated catalyst effectiveness factor in porous activated carbons (>0.99) proves that the reaction is taking place in the kinetic regime.

In heterogeneous catalytic stearic acid deoxygenation, the main product was typically *n*-heptadecane (*n*-C17); however, 1-heptadecene (1-C17) and other unsaturated C17 products (SC17) were formed in minor amounts (Figure 2).

The saturated fatty acid impurities in the stearic acid feed (98.7% purity, according to gas chromatography) are palmitic acid, $C_{15}H_{31}COOH$ (0.19%), margaric acid, $C_{16}H_{33}COOH$ (0.13%), and arachidic acid, $C_{19}H_{39}COOH$ (0.23%). As expected, the fatty acid impurities are also deoxygenated to corresponding hydrocarbons. The deoxygenation of lighter and heavier fatty acids is visualized in Figure 3 by plotting concentration of formed hydrocarbons versus the concentration of respective fatty acids, where one can see a linear correlation between palmitic acid and pentadecane as well as between margaric acid and hexadecane. Although the relationship between arachidic acid and nonadecane concentration is not as straightforward as in other cases, nonetheless, an increase of the formed amount of nonadecane is obvious as arachidic acid is converted. Note that the accuracy of the measured concentrations in this case has to be taken with precaution because of the very low concentrations.

Catalyst Screening. The catalytic deoxygenation of stearic acid was carried out over a variety of catalysts under similar reaction conditions as used in the thermal deoxygenation. Initial catalyst screening was performed to narrow the range of potential metal support combinations active and selective in the deoxygenation reaction. Additionally, a more thorough inves-

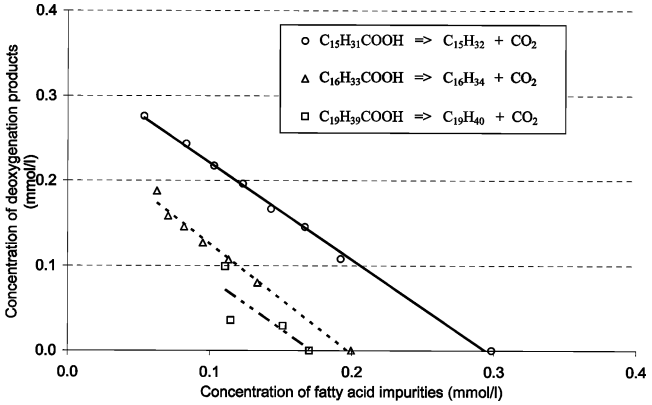

Figure 3. Concentration of formed deoxygenation products versus concentration of fatty acid impurities in the catalytic deoxygenation of stearic acid impurities; palmitic acid ($C_{15}H_{31}COOH$), margaric acid ($C_{16}H_{33}COOH$), and arachidic acid ($C_{19}H_{39}COOH$) in dodecane over 5% Pd/C.

tigation on the most promising candidates obtained from catalyst screening was done.

The deoxygenation of stearic acid was investigated over different metals (Pd, Pt, Ru, Mo, Ni, Rh, Ir, and Os) supported on carbon and metal oxides. Moreover, a Raney nickel type catalyst was tested. A summary of the catalyst screening results is shown in Table 5.

Apart from previously discussed deoxygenation reactions (reactions I−IV in section 1, reactions 1−4 in Figure 4), several other reactions (i.e., isomerization, dehydrogenation, hydrogenation, and cyclization) were observed during the catalyst-screening experiments. Not surprisingly, the deoxygenation products (*n*-heptadecane and *n*-heptadecenes) were subsequently isomerized and/or hydrogenated/dehydrogenated. Minor amounts of C17 cyclic and aromatic molecules were produced under hydrogen deficient reaction conditions (reaction 5−9, Figure 4). Furthermore lower fatty acids (C10−C17 acid) and shorter hydrocarbons (C13−C16) were formed via cracking (reaction 10). Heavier products, such as a symmetrical ketone of stearic acid as well as dimers of dehydrogenated stearic acid and unsaturated hydrocarbons, were detected (reaction 11−13), being in accordance with literature.[16−18] Although production of alcohols via acid hydrogenation is well-known over heterogeneous catalysts,[19] no direct hydrogenation to fatty alcohols was observed under these hydrogen deficit conditions.

When comparing the initial reaction rates over different catalysts, it is evident that the highest rates were obtained over supported carbon catalysts. The highest initial reaction rate was achieved over 5% Pd/C (1.9 mmol/s/g_{met}), while 1% Pd/C despite higher dispersion exhibited a somewhat lower, but still significant, rate (1.32 mmol/s/g_{met}). Presumably, the higher initial rates over carbon supported catalysts can originate from the catalyst structure, i.e., the specific surface areas which are typically larger in carbon than in silica and alumina supports, thus minimizing the effect of catalyst deactivation caused by sintering and/or coking. Another viable explanation is attributed to the carbon supports complex properties, depending on the origin of the carbon, such as amphotheric properties and different surface functional groups,[20] which can, as such, enhance the catalytic reaction. Over alumina supports, the initial rates varied substantially; over Pd and Pt on alumina, the initial reaction rates were 1 order of magnitude lower than on active carbon. Other catalysts, e.g., Ir/Al_2O_3, Ni/Al_2O_3, and NiMo/Al_2O_3, were substantially less active, whearas Ir/SiO_2 seems to have no catalytic effect, with conversion and product distribution similar to the thermal treatment. Minimal activity was observed over Ru/SiO_2 and a skeletal nickel catalyst.

Metal-supported carbon catalysts were very selective toward deoxygenation products (Table 5). All the palladium and the platinum on carbon catalysts achieved >90% selectivity toward deoxygenation products (*n*-heptadecane, 1-heptadecene, and sum of other C17 products) after 6 h. Additionally Rh, Ru, and Os on carbon catalysts exhibited relatively high selectivity toward deoxygenation products. Apart from the above-mentioned supported carbon catalysts, the following catalysts displayed high selectivity toward deoxygenation products: Ni/SiO_2 and Ni/Cr_2O_3. Moreover, the Ni/Cr_2O_3 catalyst was particularly selective toward *n*-heptadecane.

Table 5. Performance of the Screened Catalysts in the Deoxygenation of Stearic Acid (Reaction Conditions: $m_{\text{stearic acid}} = 4.5$ g, $m_{\text{dodecane}} = 86$ g, $m_{\text{catalyst}} = 1$ g, $T = 300$ °C, $p = 6$ Bar, $V_{\text{carrier gas}} = 25$ mL/min (He))

		deoxygenation selectivity, S^a (%)				side product selectivity, S^a (%)				
catalyst	conversion, X^a (%)	S_{n-C17}	S_{1-C17}	$S_{\Sigma C17}$	Total S_{C17}	S_{C18}	S_{C35}	$S_{crack}{}^b$	$S_{heavy}{}^c$	$S_{other}{}^d$
81% Raney-Ni	14.0	30	13	7	50	<0.5		17	32	
16% Ni/Al_2O_3	17.8	29	12	4	46	<0.5	12	13	29	
60% Ni/SiO_2	18.1	19	30	10	58	1		20	21	
50% Ni/Cr_2O_3	12.3	48	8	3	60			17	24	
3%,9% NiMo/Al_2O_3	8.6	15	4	3	23			3	74	
5% Ru/SiO_2	7.2	6	14	4	23		60	7	11	
5% Ru/MgO	96.2						99	−	1	
5% Ru/C	13.2	24	27	14	65	<0.5	8	11	15	
5% Pd/Al_2O_3	23.7	20	7	15	42		48	1	9	
1% Pd/C	33.4	52	6	36	94	1		1	2	2
10% Pd/C	48.1	60	5	29	94	<0.5	3	1		2
5% Pd/C	100.0	95	0	3	99			1		<0.5
8%,2% PdPt/C	61.6	73	7	15	96	<0.5		3	1	<0.5
5% Pt/Al_2O_3	19.9	18	17	11	46	<0.5	37	2	14	<0.5
5% Pt/C	86.0	87	1	7	95	<0.5		4	<0.5	<0.5
2% Ir/Al_2O_3	17.2	1	1		2		85		12	
1% Ir/SiO_2	4.6	14	29	26	69			2	29	
5% Os/C	6.9	29	15	9	53		17	7	22	
3% Rh/SiO_2	15.7	7	9	7	23		56	3	18	
1% Rh/C	17.9	18	13	53	85	<0.5	4	4	7	<0.5

[a] Conversion of stearic acid and selectivities toward products after 6 h of reaction. [b] Crack denotes cracking products consisted of shorter fatty acids, C10−C17 acids ,and shorter hydrocarbons, C13−C16 hydrocarbons. [c] Heavy denotes dimeric products formed via unsaturated acids and olefins. [d] Other denotes unidentified products.

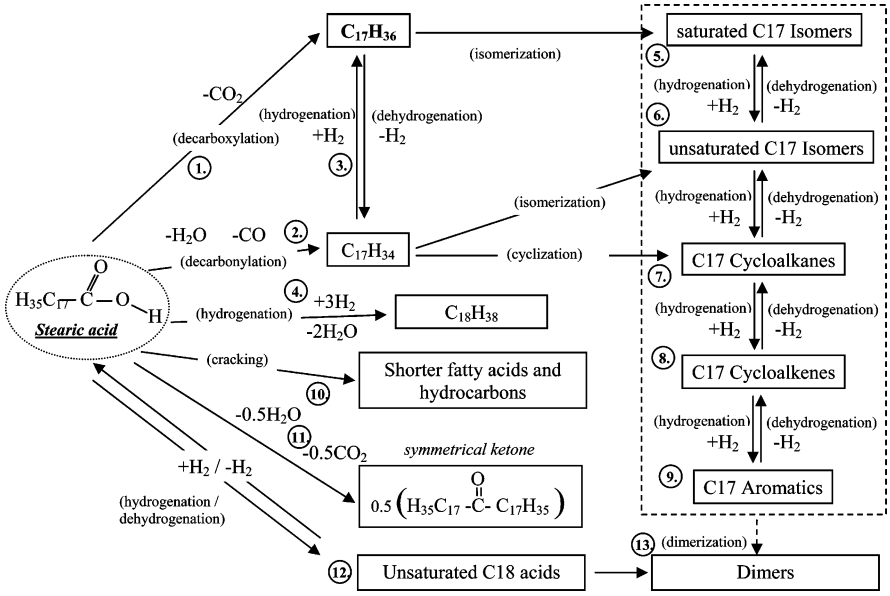

Figure 4. Tentative reaction routes of stearic acid over heterogeneous catalyst at 300 °C under inert atmosphere.

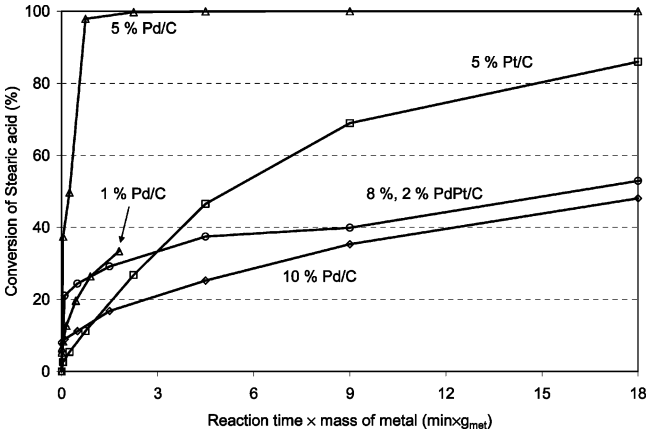

Figure 5. Conversion of stearic acid in the deoxygenation reaction over Pd and Pt supported catalysts. Reaction conditions are the same as in Figure 2.

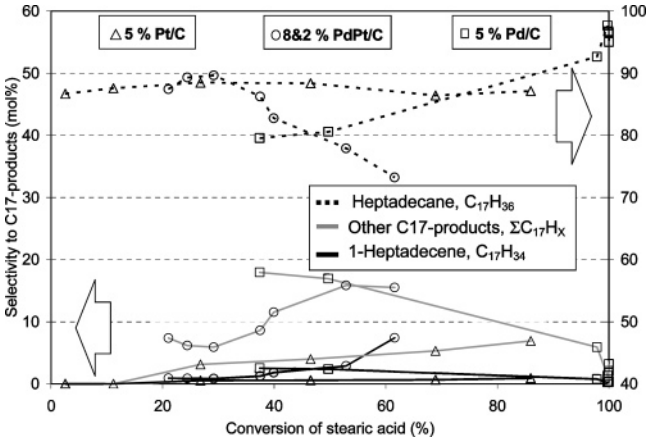

Figure 6. Product selectivities vs stearic acid conversion in the deoxygenation reaction over Pd and Pt catalyst. Reaction conditions are the same as in Figure 2.

Detected side products were the hydrogenation product, C18-hydrocarbons (C18), and the symmetrical ketone (C35) of stearic acid. Furthermore, cracking and dimeric products were detected; the cracking products consisted of shorter fatty acids, C10−C17 acids and shorter hydrocarbons, and C13−C16 hydrocarbons, while dimeric products were formed via unsaturated acid dimerization and olefin metathesis. Some minor traces of unidentified products (other) were observed. Selectivities toward side products after 6 h are tabulated in Table 5.

The hydrodeoxygenation product C18 hydrocarbons were only detected in minor amounts (<2%) over Ni, Pt, and Pd catalysts. The production of the symmetrical ketone was observed over several catalysts. Especially over Ru/MgO, the symmetrical ketone was the major product formed, corresponding to a selectivity >99%. In addition to Ru/MgO, the ketonization of stearic acid was catalyzed by Ir/Al_2O_3, Pd/Al_2O_3, Pt/Al_2O_3, Ru/SiO_2, and Rh/SiO_2, giving significant selectivities to formation of ketone. The selectivity to cracking for all screened catalysts is relatively low (0−11%), with the exception of nickel catalysts. Ni/SiO_2 had the highest selectivity toward cracking, whereas Raney Ni, Ni/Cr_2O_3, Ni/Al_2O_3, and $NiMo/Al_2O_3$ had somewhat lower cracking selectivities. The formation of heavier products, such as dimers, were profound over nickel catalyst. $NiMo/Al_2O_3$ catalyst exhibited the highest selectivities toward heavier products, while the selectivity for Raney Ni, Ni/Al_2O_3, Ni/SiO_2, and Ni/Cr_2O_3 was ∼2× less. The higher heavy product selectivities over nickel catalysts are partially due to a larger extent of cracking and, consequently, a subsequent olefin metathesis to dimers. Unidentified products were mainly observed over active Pt and Pd catalysts, although in trace amounts (<2%).

Catalyst stability toward deactivation could be related to the amount of unsaturated products (unsaturated deoxygenation and cracking products), further leading to catalyst coking. This assumption corresponds well with experimental data, i.e., 8 % Pd, 2 % Pt /C is relatively stable during the reaction and exhibited, at the same time, a low selectivity to unsaturated products, whereas Ru/C and Rh/C catalysts strongly deactivated, being selective toward unsaturated products. Additionally, the Ru/MgO catalyst, which was selective toward ketone, was very stable, giving 96% conversion of stearic acid after 6 h.

Catalytic Deoxygenation of Stearic Acid over Pd and Pt Supported Carbon Catalysts. A more extensive investigation of Pd and Pt supported carbon catalyst was conducted. As mentioned previously, the carbon catalysts supported were typically very active and selective during the deoxygenation reaction (Table 5).

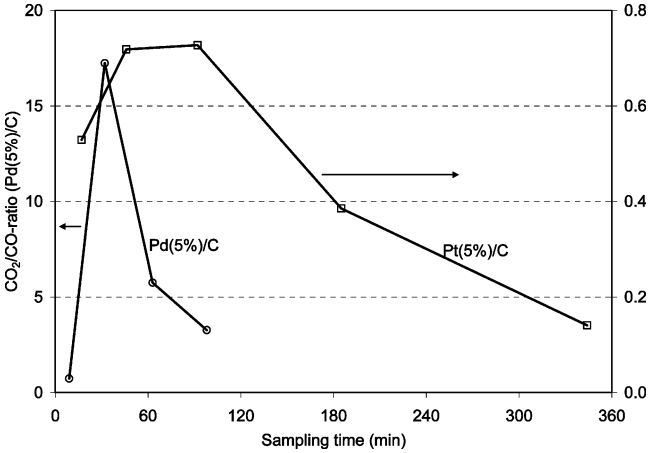

Figure 7. The results of CO_2/CO ratio as a function of sampling time over 5% Pd/C and 5% Pt/C catalysts. Reaction conditions are the same as in Figure 2.

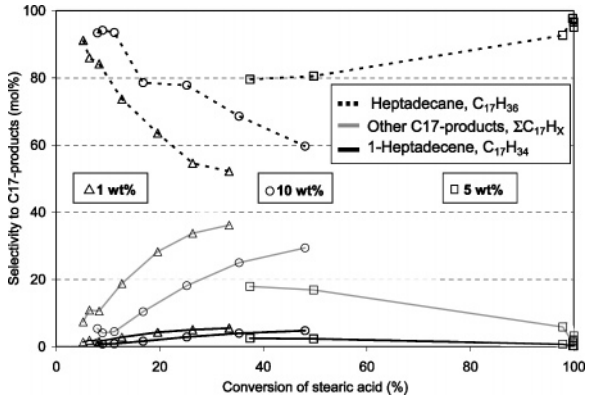

Figure 8. The effect of metal loading on formation of deoxygenation products over Pd/C catalysts. Reaction conditions are the same as in Figure 2.

Interestingly the initial reaction rate was significantly higher over the palladium and the bimetallic catalysts than over the platinum one (Figure 5).

Conversion of stearic acid over palladium yielded primarily heptadecane, selectivity to which increased as a function of conversion (Figure 6). However, over the bimetallic catalyst, the formation of heptadecane decreased with conversion, while formation of other C17 products was increasing (Figure 6). The product distribution over the platinum catalyst was almost independent of conversion, with ~85% selectivity toward heptadecane (Figure 6). The increase of selectivity toward other (unsaturated) C17 products over the bimetallic catalyst compared to the product distribution over the platinum catalyst might explain the more rapid catalyst deactivation observed in the former rather than the latter case (Figures 5 and 6).

Gas-phase analysis gave an indication that the dominating process over palladium catalyst was stearic acid decarboxylation, whereas over platinum, the decarbonylation reaction was more profound, since the CO_2/CO ratio over the former catalyst was >17, whereas for the latter catalyst it was <1 (Figure 7). The very active palladium catalyst had CO_2/CO ratio >15 at 30 min of sampling time. It should be pointed out that the gas-phase sampling time is delayed by ~20 min compared to reaction time.

The effect of palladium metal loading was investigated by conducting experiments with 1, 5, and 10 wt % palladium supported on carbon (Figure 5). The characterization by N_2 physisorption, CO chemisorption, and H_2 TPD did not provide an explanation for the observed order of the catalytic activities. Nevertheless, the correlation of the activity with acidity of the aqueous catalyst slurry indicates that slightly alkaline properties are preferred (Table 3). Furthermore, when comparing the initial reaction rates of stearic acid with the conversions of stearic acid after 6 h of reaction over 1% Pd/C and 5% Pd/C, it was observed that the catalyst deactivated stronger in the former case, while the latter tends to be more stable during the reaction.

Investigating the effect of palladium loading on product selectivity showed that the formation of heptadecane was higher over 5% palladium than over 1% and 10% palladium. The selectivity toward heptadecane increased as a function of the conversion over 5% palladium catalyst, while declining selectivity to heptadecane is observed over the 1% and 10% palladium catalysts (Figure 8). Simultaneously, the more pronounced formation of other C17 products, mainly unsaturated ones, might cause catalyst coking and explain the diminished activity of the latter catalyst compared to 5% Pd/C.

Conclusions

A heterogeneous catalytic method for production of diesel fuel hydrocarbons was developed. It is based on deoxygenation reactions, e.g., decarboxylation and/or decarbonylation reactions, where the renewable raw materials, i.e., stearic acid, are converted to diesel fuel compounds, carbon dioxide, and/or carbon monoxide. The catalytic deoxygenation of stearic acid over heterogeneous catalysts was successfully achieved with high activity and selectivity to the desired product, heptadecane. Even though this reaction can be effectively performed over a variety of catalysts, the catalyst screening results revealed that the reaction is preferably carried out over palladium and platinum supported on activated carbons. Furthermore, the gas-phase analysis demonstrated that the decarboxylation reaction was more profound over the Pd/C catalyst, while the decarbonylation reaction was more evident over the Pt/C catalyst. The outcome of comparison with different metals on the equivalent supports by normalizing the results with metal content depicted that the beneficial effect of a metal in the deoxygenation reaction is in the decending order Pd, Pt, Ni, Rh, Ir, Ru, and Os. Apart from deoxygenation reactions, other reactions, such as hydrogenation, dehydrogenation, cyclization, ketonization, dimerization, and cracking, were observed in various extents depending on the catalysts.

Acknowledgment

This work is part of the activities at the Åbo Akademi Process Chemistry Centre (ÅA-PCC) within the Finnish Centre of Excellence Programs appointed by the Academy of Finland (2000−2011). Financial support from the national funding agency for technology and innovation, TEKES, is gratefully acknowledged. The authors express their gratitude to Mr. Markku Reunanen for his contribution to GC−MS analysis and Dr. Natalja Kul′kova for catalyst preparation.

Supporting Information Available: The supporting information includes typical chromatograms of liquid-phase and gas-phase mixtures, details of the effect of internal diffusion in porous activated carbon catalysts, and a table of calculations of internal mass transfer at given reaction conditions. This material is available free of charge via the Internet at http://pubs.acs.org.

Literature Cited

(1) Srivastava, A.; Prasad, R. Triglyceride-Based Diesel Fuels. *Renewable Sustainable Energy Rev.* **2000,** *4*, 111−133.

(2) Lee, R.; Pedley, J.; Hobbs, C. Fuel Quality Impact on Heavy-Duty Diesel Emissions—A Literature Review. *SAE Pap. 982649* **1998**.

(3) Demirbas, A. Biodiesel from Vegetable Oils via Transesterification in Supercritical Methanol. *Energy Convers. Manage.* **2002**, *43*, 2349−2356.

(4) Fangrui, M. A.; Milford, H. Biodiesel Production: A Review. *Bioresour. Technol.* **1999**, *70*, 1−15.

(5) Fukuda, H.; Kondo, A.; Noda, H. Biodiesel Fuel Production by Transesterification of Oils. *J. Biosci. Bioeng.* **2001**, *91*, 405−416.

(6) Idem, R. O.; Katikaneni, S. P. R.; Bakhshi, N. N. Catalytic Conversion of Canola Oil to Fuels and Chemicals: Roles of Catalyst Acidity, Basicity and Shape Selectivity on Product Distribution. *Fuel Process. Technol.* **1997,** *51*, 101−125.

(7) Leung, A.; Boocock, D. G. B.; Konar, S. K. Pathway for the Catalytic Conversion of Carboxylic Acid to Hydrocarbons over Activated Alumina. *Energy Fuels*, **1995**, *9*, 913−920.

(8) Kubičková, I.; Snåre, M.; Mäki-Arvela, P.; Eränen, K.; Murzin, D. Yu. Hydrocarbons for Diesel Fuel via Decarboxylation of Vegetable oils. *Catal. Today* **2005**, *106*, 197−200.

(9) Bertram, S. H. De werkung van selenium op stearinzuur. *Chem. Weekblad* **1936**, 457−459.

(10) Foglia, T. A.; Barr, P. A. Decarbonylation Dehydration of Fatty Acids to Alkenes in the Presence of Transition State Metal Complexes. *J. Am. Oil Chem. Soc.* **1976**, *53*, 737−741.

(11) Maier, W. F.; Roth, W.; Thies, I.; v. Rague Schleyer, P. Gas-Phase Decarboxylation of Carboxylic Acids *Chem. Ber.* **1982**, *115*, 808−812.

(12) Stern, R.; Hillion, G. Process for Manufacturing a Linear Olefin from a Saturated Fatty Acid or Fatty Acid Ester. U.S. Patent 4,554,397, 1985.

(13) Parmon, V. N. Catalytic Technologies for Energy Production and Recovery in the Future. *Catal. Today* **1997**, *35*, 153−162.

(14) Bernas, A.; Kumar, N.; Mäki-Arvela, P.; Kul'kova, N.; Holmbom, B.; Salmi, T.; Murzin, D. Yu. Isomerization of Linoleic Acid over Supported Metal Catalyst. *Appl. Catal., A.* **2003,** *245*, 257−275.

(15) Markus, H.; Mäki-Arvela, P.; Kumar, N.; Heikkilä, T.; Lehto, V.-P.; Sjöholm, R.; Holmbom, B.; Salmi, T.; Murzin, D. Yu. Reactions of Hydroxymatairesinol over Supported Palladium Catalyst. *J. Catal.* **2006**, *238*, 301−308.

(16) Pestman, R.; Koster, R. M.; van Duijne, A.; Pieterse, J. A. Z.; Ponec, V. The Formation of Ketones and Aldehydes from Carboxylic Acids, Structure−Activity Relationship for Two Competitive Reactions. *J. Catal.* **1997**, *168*, 265−272.

(17) Sugiyama, S.; Sato, K.; Yamasaki, S.; Kawashiro, K.; Hayashi, H. Ketones from Carboxylic Acids over Supported Magnesium Oxide and Related Catalysts. *Catal. Lett.* **1992**, *14*, 127−133.

(18) Goebel, C. G. Method for Manufacturing Polymerized Fatty Acids. U.S. Patent 2,664,429, 1953.

(19) Augustine, R. L. *Heterogeneous Catalysis for the Synthetic Chemist*; Marcel Dekker: New York, 1996; p 462.

(20) Perä, M. Activated Carbon as a Catalyst Support. In *Industrial Chemistry Publications Series*; Helsinki University of Technology: Helsinki, Finland, 1995.

Received for review March 20, 2006
Revised manuscript received May 26, 2006
Accepted May 26, 2006

IE060334I